

PIV Visualization of Acoustic Streaming in Non-Newtonian Fluid

Herimonja A. Rabenjafimanantsoa¹, Barbara M. Wrobel¹, and Rune W. Time¹

¹ University of Stavanger, Norway

ABSTRACT

Acoustic streaming produced by ultrasonic transducers is experienced in highly viscous fluid. Polyanionic Cellulose (PAC) has been used as fluid medium. The streaming at the near field of the transducer was easily noticeable using colour indicator. High speed camera has been used for visualization and quantification of the streaming velocity. A method for determining acoustic streaming in a static viscous fluid medium is described in this article. As expected that the velocity of the streaming increased with the adjusted voltage.

INTRODUCTION

Acoustic streaming has been widely applied for non-invasive intervention purposes, both in industry and medicine. It has been utilized for mixing of chemical solutions¹, mixing of laminar flow by inducing vortex flows in microchannels² and breaking up kidney stones³ and other small scale applications that require external treatment.

Acoustic streaming is expected to be vigorous in low viscosity, water-like fluids with suspensions of similar viscosity⁴. However it is expected to be more challenging in case of highly viscous non-Newtonian fluids due to their great sound attenuation properties.

In this paper, we study streaming effect in a non-Newtonian viscous water-Polyanionic Cellulose (PAC) solution as a

function of various polymer concentrations, as well as on applied voltage.

Particle image velocimetry, PIV, is a technique which among others is available for measuring acoustic streaming. This technique is based on video images of an illuminated fluid flow using seeding particles. The velocity profile can be reconstructed in real time in two or three dimensions. Rabenjafimanantsoa et al.⁵ applied a 4 MHz transducer from Metflow⁶ in their study. Provided that generally, the dynamic of the ultrasonic beam emit strong signals, as photographed in Fig. 1, it is highly necessary to measure the streaming field.

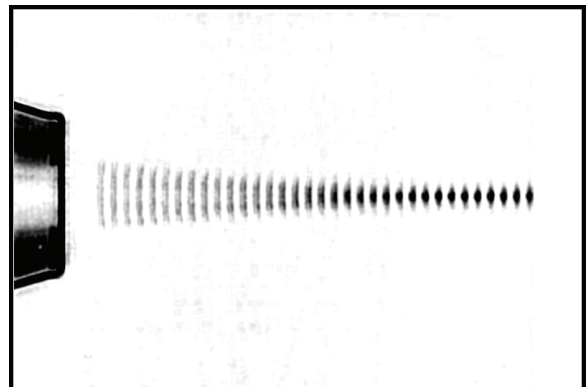


Figure 1. Schlieren image of pulse train for 15-MHz focused transducer⁷. The image is inverted for clarity. The transducer is emitting sound from the left to a near field and far field regions.

As seen from Fig. 1, the focused transducer emits acoustic sound which is

transmitted into the fluid with different properties in the "near" and "far" regions. The near field region is irregular with a narrow "waist". The far field beam can be characterized nearly as parallel flat wave beamfront with a slight beam divergence.

MATERIALS AND METHODS

Fig. 1 shows a schematic representation of the experimental setup. It consists of a camera, illumination system and an acoustic transducer.

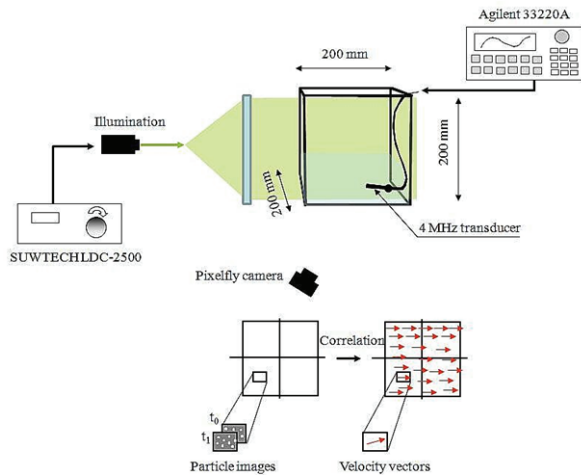


Figure 2. Overview of the experimental setup, which consists of a camera, a laser source, and an acoustic transducer.

The container 200x200x200 mm and glass plate were assembled together to form a squared section. This was chosen to fulfil the optical condition. We used a 4 MHz transducer from Metflow⁶ having 5 mm in diameter and immersed in the water container. The probe is powered with a 20 MHz Function/Arbitrary Waveform Generator model 33220A from Agilent Technologies.

Our PIV system consists of a laser diode D PGL-22006 which is controlled by a Suwtech LDC-2500 allowing from 0 to 2.5 A supplying a thick lasersheet and a camera. To narrow the laser beam a collimator made of black nylon sheets was set between the laser and the glass plate. The high speed camera is a computer controlled Pixelfly

from Cooke Corporation, 1392x1024 pixels and is able to record double instant images using CamWare 2.13 software. A 105 mm lens was used

The PIV technique was well described by Rabenjafimanantsoa et al.⁵ but we recall it here for brevity. The PIV consists of capturing two flashed exposures using a high speed camera. These images are divided into small subwindows (32x32 pixels), interrogation areas, as illustrated in Fig. 2.

During Δt which is the time between two consecutive images (65.5 ms), a single particle has moved to a displacement Δs . The absolute velocity is then computed as $\Delta s/\Delta t$, and the vector is along Δs . When using water additional seeding particles was necessary. These are neutral buoyant particles, density 1.05 kg/dm³ and size 63-80 μm from Grilltex, EMS-Chemie AG Switzerland.

Two different concentrations of polyanionic cellulose, PAC regular were used: 50 and 400 ppm dissolved in water. We used the same procedure as described in Rabenjafimanantsoa et al.⁵ but for brevity we recall the methods. The Silverson mixer model LART-A at 1500 rpm was used for preparation of the solution before pouring into the container. The rheological measurements were taken using a Physica UDS 200 rheometer with the concentric cylinder configuration Z3 DIN. We measured the samples at 21°C with decreasing shear rates.

No additional seeding of particles was needed since the polymer particles were sufficient to be used as tracer particles. Therefore in some cases, even though seeding is not completely homogeneous, it is dense enough to allow full analysis.

The viscosity measurements were taken before the tests have been run. The results from the viscosity measurements will be presented later. The same experimental system as used by Rabenjafimanantsoa et al.⁵ was set up during this run. These were

taken since during the experiments the acoustic transducer was defected leaving us results from preliminary tests. Lissamine red 6B from Chroma-Gesellschaft GmbH was used for visualization.

EXPERIMENTAL PROCEDURES

Acquired images from the pixelfly camera were imported in DynamicStudio⁸ (version 2.10) for postprocessing.

Fig. 3 shows a typical example of such cross correlation. The velocity vectors are represented by arrows in the horizontal and vertical plane. Furthermore, these velocities are anchored and plotted at their tail points. From the horizontal plane, every third vector with zero offset is shown, as clearly seen in Fig. 3.

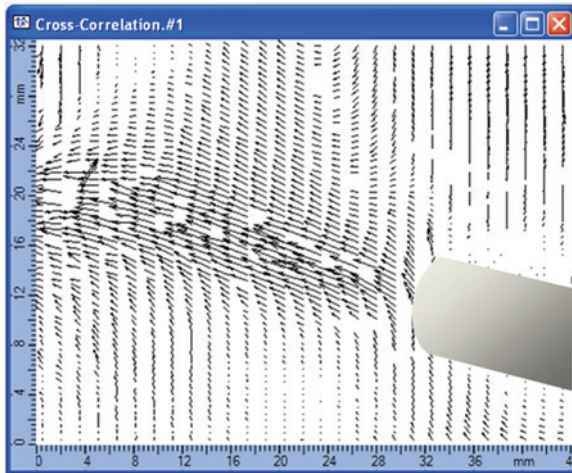


Figure 3. PIV picture showing the velocity vectors anchored at every third vector in the horizontal plane. The transducer has been drawn manually.

The next step is to plot the velocity values along a line, as shown in Fig. 4. This is necessary for comparison of the acoustic streaming in fluid medium as a function of rheology and voltage intensity.

Then a coherence filtering (modified median filter) was applied to the results from cross correlation. This acts as an “error removal” filter because it modifies a

velocity vector if it is inconsistent with the dominant surrounding vectors⁷.

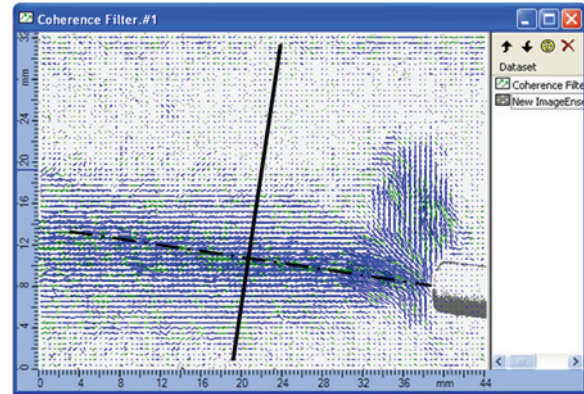


Figure 4. PIV picture showing the filtered cross correlation vector plot superimposed by the image. The transducer's beam path and the line where the profile plots are extracted from is shown as a discontinuous line.

Fig. 4 also shows an example from such filtering method. No additional seeding of particles was needed since the polymer particles were sufficient to be used as tracer particles.

Finally, the comparison of the velocity profiles will be made along the line that is perpendicular to the beam line. This line is situated approximately at 20 mm parallel to the transducer face. This is represented by the dashed line, as seen in Fig. 4. This figure is a superposition of the image and the resulted cross correlation process. It is then necessary to extract profiles from U and V components. This extracted velocity is given by:

$$L = \sqrt{U^2 + V^2} \quad (1)$$

where U is the velocity in the horizontal direction and V in the vertical direction.

RESULTS AND DISCUSSIONS

Streaming in water

Acoustic streaming results from water are already presented in Figs. 3 and 4. In

these figures only the velocity vectors are shown. In Fig. 5 the acoustic streaming is quantified by the length of the vector components. The x-axis shows the distance from the transducer face along the jet centreline. The y-axis is velocity vector length.

It can be seen that as the amplitude levels (2, 5 and 7.5 Volts) is increased the length of the vectors, and hence the acoustic streaming, is increased accordingly. The maximum speed along the jet centerline is observed around 10 mm from the transducer face.

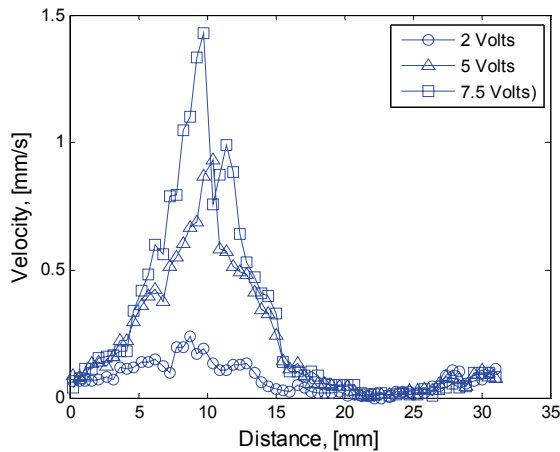


Figure 5. Profile plots from 2, 5 and 7.5 Volts.

The profile plot from 2, 5 and 7.5 Volts are plotted together. It is seen that the acoustic streaming is strongest where the beam intensity is highest, as seen in Fig.1. This is around distance 10 mm from the transducer face. Similarly the streaming is strongest in, and along, the beam axis. The maximum length for the 7.5 Volt is 1.4 mm/s at 9.8 mm. The velocity profile in the beam axis is relatively symmetrical and has its maximum at the centre.

In Fig. 6 Lissamine red 6B was deposited with syringe in the fluid. The arrow indicates the ultrasonic beam direction. It can be seen that the stripes are deformed by the acoustic pressure.

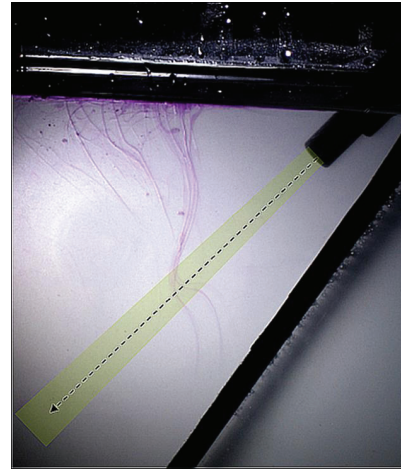


Figure 6. Visualization of acoustic streaming generated at 10 V charging. The stripes are deformed by acoustic pressure. Glycerine was used as fluid medium.

The deformation is easily noticeable. The voltage charging was set to 10 Volts.

Streaming in polymeric solution

The viscosity measurement of the PAC solutions is shown in Fig. 7.

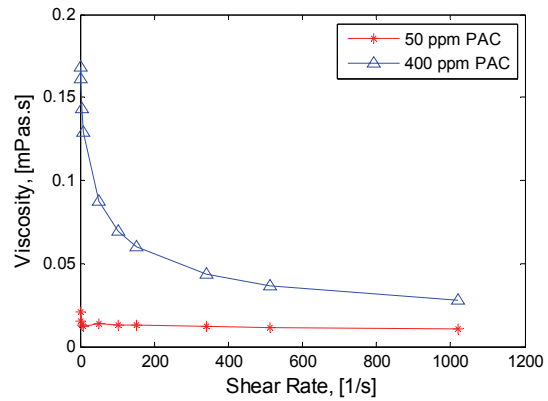


Figure 7. Viscosity versus shear rate at 21 °C of the 50 and 400 ppm concentrations of PAC dissolved in water.

Unfortunately, the 4MHz ultrasonic transducer malfunctioned during the non-Newtonian runs. Nevertheless, a qualitative result is presented. And considering that the emphasis of this paper was to visualize the acoustic streaming in non-Newtonian fluid, some observations from our runs are shown.

These observations are considered to be generally valid since theory suggests that non-Newtonian fluid greatly attenuates sound⁴.

In Fig. 8 Lissamine red 6B was also deposited in the same way as seen in Fig. 6, with syringe to visualize streaming in the viscosified fluid. For clarity the arrow that indicates the ultrasonic beam direction is also shown in Fig. 6. It can be seen that the deposited stripes in Fig. 8 are also deformed by the acoustic pressure but in a lesser magnitude. The noticeable peak is no longer shown. This could suggest the attenuation of the acoustic streaming, as expected.



Figure 8. Acoustic streaming in 400 ppm PAC dissolved in water.

Despite difficulties in quantifying the velocity profiles using PAC due to the malfunction of the transducer, a reasonable relationship with the solution between non-Newtonian and Newtonian fluids can be argued. The centrally acoustic beam peak might actually be smoothed in non-Newtonian case.

Comparison of Figs. 6 and 8 shows qualitatively the difference in the acoustic damping. In the direction of the beam axis velocity is expected to show strong streaming. This is not the case in Fig. 8 which may suggest that the sound pressure might have been attenuated greatly using 400 ppm PAC dissolved in water as fluid medium.

Care should be taken in observing the streaming as it sets up large scale circulations in the enclosed tank. The circulations eventually interact back and modify the streaming jet.

CONCLUSION

Experiments were conducted to visualize acoustic streaming produced by a 4 MHz transducer in Newtonian and non-Newtonian fluid. PIV technique was used for quantification of the streaming velocity. The features of the streaming velocity maps were shown. The streaming is highest in the beam centerline.

As expected the maximum peak velocity along the transducer beam is in the axial position. At this region the streaming is highest as the intensity of charging voltage is increased. The velocity profile in the beam axis is relatively symmetrical as would be expected for a good quality transducer.

A comparison of the streaming pattern in the different fluids also reveals that there exists a peak velocity at a certain distance from the transducer face. This is seen especially in Newtonian fluid. The magnitude of this feature depends on applied transducer voltage and viscosity.

ACKNOWLEDGEMENTS

The authors acknowledge the support from The Research Council of Norway through the CLIMIT project nr. ES422910.

REFERENCES

1. Suri, C., Takenaka K., Yanagida H., Kojima Y., and Koyama K. (2002), "Chaotic mixing generated by acoustic streaming", *Ultrasonics*, **40**, 393-396.
2. Bengtsson M. and Laurell T. (2003), "Acoustic streaming – ultrasonic agitation in microchannels", ^{7th} *International Conference on Miniaturized Chemical and Biochemical Analysis Systems*, Squaw Valley, California USA.

3. Choi M.J., Doh D.H., Cho K.S., Paeng D.G., Ko N.H., Kim K.S., Rim G.H., and Coleman A.J. (2004), "Visualization of acoustic streaming produced by lithotripsy field using a PIV method", *J. Phys.: Conference Series*, **1**, 217-223.
4. Wu J. and Nyborg W. (editors), (2006) "Emerging Therapeutic Ultrasound", World Scientific, USA, pp. 28-29, 43-38
5. Rabenjafimanantsoa, A.H., Time, R. and Saasen A. (2007), "Characteristic of the velocity profiles over fixed dunes in pipe", *Ann. Trans. Nordic Rheol. Soc.*, **14**, 141-147
6. Met-Flow (2000), "UVP Monitor Model XW. User's guide", Switzerland
7. Schneider, B. and Kirk Shung, K. (1996), "Quantitative analysis of pulsed ultrasonic beam patterns using a Schlieren system", *IEEE Transactions on Ultrasonics, Ferroelectrics, and Frequency Control*, **43**, 6, 1181 - 1186
8. DynamicStudio software version 2.10.86, DantecDynamics A/S